Poly(ethylene oxide): Electronic Structure, Energetics, and Vibrational Spectrum

Robson Pacheco Pereira,*,†,‡ Ana Maria Rocco,‡ and C. E. Bielschowsky†

Grupo de Espectroscopia Teórica, and Grupo de Materiais Condutores, Instituto de Química, Universidade Federal do Rio de Janeiro, CT, Bloco A, Cidade Universitária, Rio de Janeiro, RJ, 21945-970, Brazil

Received: March 29, 2004; In Final Form: June 18, 2004

The electronic structure, energetics, and vibrational spectrum of poly(ethylene oxide) (PEO) are determined from density functional theoretical calculations on model systems $(CH_2CH_2O)_nX_2$, $((EO)_nX_2)$, where X is a termination group, such as methyl or hydroxyl, and *n* varies from 2 to 8. Geometry optimization was performed on these linear model systems chosen to represent the noncrystalline conformer of PEO, and the convergence of selected properties (total energy, vibrational spectra) was studied. To simulate the crystalline conformer, geometry optimization and vibrational spectrum calculations were carried out on a helical $(EO)_6(CH_3)_2$ model system. Differential scanning calorimetry data were employed to determine the crystalline fraction, used as weight for the simulation of total vibrational spectra, based on the spectra of the two conformers. The high resolution simulated spectra exhibited the contribution of individual vibrational modes to the experimentally observed broad peaks (or envelopes), while the simulated spectra with low resolution exhibited good agreement with experimental data, indicating a strong influence of the line width on the simulated spectra, caused by the distribution of chain conformations in the experimental PEO sample. The electronic structure of the linear $(EO)_6(CH_3)_2$ model system exhibited localization of the frontier orbitals on the oxygen atoms, where the border effect is highly pronounced, the orbitals localized on the oxygen atoms closer to the termination being highly energetic. The simulation of PEO by the finite size cluster approach utilizing oligo(ethylene oxide) model systems with six units was shown to be a good approximation to the calculation of electronic structure and vibrational spectra.

1. Introduction

Many group I and II metal salts may be dissolved in solid coordinating polymers such as poly(ethylene oxide) (PEO), resulting in the preparation of polymeric solid electrolytes (PSE). Such materials may be considered as coordination compounds lying somewhere between classical coordination chemistry and solid-state chemistry.[1] When lithium salts are employed, the resulting materials uniquely combine solid yet flexible mechanical properties with ionic conductivity. This combination holds the key to the development of solid-state electrochemical devices such as rechargeable lithium batteries,[2] artificial muscles, and electrochromic display devices,[3] in which a film of the material is used as the electrolyte.

One of the most commonly used analytical techniques for analysis of PSE is vibrational spectroscopy. This is especially true for probing the occurrence of ion pairs or higher aggregates,[4,5] all of which lower the number of effective charge carriers in the PSE, and/or for detecting crystallinity of polymeric matrixes based on PEO blends.[6,7] Generally, there has been an experimental focus on the development and characterization of electrolytes for lithium polymer battery purposes. However, theoretical descriptions have been gaining attention in the recent literature.[8]

According to literature reports, the ethers (hard bases) are expected to bind strongly to alkali metals (hard acids), resulting in higher ionic conductivities.[9] Not only the types of electronegative centers but also the interspacings are important to the coordination strength; e.g., $(CH_2O)_n$ (PMO) and $(CH_2CH_2CH_2O)_n$ (PTMO) are both poorer coordinating solvents than PEO $((CH_2CH_2O)_n)$.[10] Further differences could also result, if other donor atoms, i.e., N or S, are present in the polymeric chain.

Johansson and co-workers[11] reported results of Hartree−Fock calculations on oligo(ethylene oxide)/Li^+ for the description of the ionic transport in helical PEO. In their work, a methyl-end-capped ethylene oxide oligomer was used as the model system and the coordination and transport of Li^+ were described. More recently, Krishnan and Balasubramanian[12] described the low-frequency vibrational spectrum of PEO using molecular dynamics simulations.

However, studies concerning the convergence of molecular properties with the chain length of ethylene oxide oligomers by quantum chemical calculations are not found in the literature to our knowledge. In the present work, we report a systematic study of the molecular properties of ethylene oxide model systems by DFT calculations, in order to describe the wave function, molecular orbitals, and theoretical vibrational spectrum of PEO.

2. Experimental Section

2.1. Materials and Sample Preparation. PEO ($M_w = 2 \times 10^6$ g/mol) was supplied by Aldrich Chemical Co. PEO was utilized after drying at 60 °C overnight but without further purification. PEO was dissolved in methanol (Merck, PA) and the solution was stirred for 24 h under dry argon atmosphere at

* Corresponding author. Fax: (55) (21) 2562-7559. E-mail: rpacheco@iq.ufrj.br.
† Grupo de Espectroscopia Teórica.
‡ Grupo de Materiais Condutores.

10.1021/jp048625x CCC: $27.50
Published on Web 07/31/2004

$$H_3C\text{-}(CH_2\text{-}CH_2\text{-}O)_n\text{-}CH_3$$

$$HO\text{-}(CH_2\text{-}CH_2\text{-}O)_n\text{-}OH$$

Figure 1. Model systems chosen to represent the oligomers of ethylene oxide.

35 °C. Films were prepared by casting from the solution on KBr pellets and dried to constant weight in a desiccator under vacuum.

2.2. Differential Scanning Calorimetry. To evaluate the thermal behavior of the PEO sample, differential scanning calorimetry (DSC) measurements were performed on a General V4.1C DuPont 2100 apparatus. The apparatus was calibrated with an indium standard under nitrogen atmosphere.

The PEO sample was first heated from 25 to 100 °C at a heating rate of 10 °C/min (run I). After a 5 min isotherm, the sample was cooled to −100 °C at the same rate (run II) and then heated at 10 °C/min to 100 °C (run III). Sample size was 5 mg, and the DSC measurements were performed in sealed aluminum pans under a N_2 flow rate of 50 mL/min. The melting temperature (T_m) and apparent melting enthalpy (ΔH_m) were determined from the DSC endothermic peak on the second heating run, and the glass transition temperature (T_g) was estimated as the midpoint of the transition. The melting enthalpy and temperature were derived from the area and the maximum of the endothermic peak, respectively. The degree of crystallinity was calculated from the following equation:

$$X_c = \frac{\Delta H_m}{\Delta H^\circ_{PEO}} \quad (1)$$

where ΔH_m is the apparent melting enthalpy per gram of PEO, and ΔH°_{PEO} is the heat of melting per gram of 100% crystalline PEO, 188 $J \cdot g^{-1}$.[13]

2.3. Infrared Spectroscopy. Infrared spectra (FTIR, Nicolet-760) were determined in the range of 400−4000 cm^{-1} at room temperature with 1 cm^{-1} resolution, 128 scans, and optimized gain.

3. Computational details

Density functional theory (DFT) calculations were carried out on the model systems represented in Figure 1. The convergence of the electronic structure and properties with the size of the representative oligomers (n) was carefully studied and is presented in section 4.2.

The calculations were carried out using the 6-31G(d,p) standard basis set for all atoms, along with the gradient-corrected DFT method, Becke3−Lee−Yang−Parr, (B3LYP).[14] Vibrational frequency calculations were performed at this level of theory to confirm that the structures obtained were true minima and to investigate the vibrational spectra of the model systems. All the calculations were performed using GAMESS.[15] To describe the localization of the molecular orbitals in the model systems, calculations with Foster−Boys (F−B)[16] and Edmiston−Ruedenberg (E−R)[17] localization were performed. For the vibrational spectrum, all the frequencies were scaled, using an ω factor of 0.9614, as suggested by Scott and Radom[18] due, in great part, to anharmonicity correction. For the simulation of vibrational spectra and possible comparison with experimental data, the calculated frequencies and intensities were "dressed" with Gaussian functions and summed along the frequency range, by use of Scilab 2.7.[19]

PEO is a polymer that presents a solid-state structure formed by chains in the helical and a range of other conformations, up to a planar conformer. From the DSC results, it was possible to calculate the crystallinity fraction and to use this value as a parameter for the scaled sum (the weights of the two conformations) of the theoretically calculated spectra. To compare the theoretical and experimental spectra, the helical conformation (TTGTTG) was chosen to represent the crystalline fraction and the linear (planar) model to represent the noncrystalline one with weights of 0.74 and 0.26, respectively, as described in section 4.1 (Thermal Analysis). This approach enables the interpretation of the PEO vibrational spectrum with details covering the two different conformations used, representing both the crystalline and noncrystalline fractions. The line widths employed were chosen to represent different "resolutions", from a finer line width (5 cm^{-1}) to a coarse one (50 cm^{-1}). The finer line width allows us to interpret the experimental spectrum as "envelopes" composed by the sum of different modes on the two conformations chosen, and the coarser line width gives a more graphical interpretation of the experimental vibrational spectrum. The refinement of the description of the infrared spectra involving two $(EO)_6(CH_3)_2$ conformations (helical and linear) was done by analyzing the vibrations of the isolated molecules and excluding the modes which involve the methyl end groups, in order to avoid border effects that could compromise the results of the simulated spectra. There were 27 and 33 vibrational modes associated with border effects in the linear and helical conformers, respectively.

This study does not cover all the possible conformations of these highly flexible systems, and to find all of these would be a truly demanding task. Still, we believe our selection of model systems provides results that are relevant to the comparison of possible structures and to the complete set of stable conformations.

TABLE 1: Thermal Properties of PEO Films Obtained by DSC

T_g	-48 °C
ΔT_g	6.1 °C
ΔC_p	2.6×10^{-2} $J \cdot g^{-1} \cdot °C^{-1}$
T_m	74 °C
ΔH_m	139 $J \cdot g^{-1}$
X_c	74%

4. Results and Discussion

4.1. Thermal Analysis. From the analyses of the DSC curves, thermal properties of PEO films were obtained and are shown in Table 1, where T_g is the glass transition temperature; ΔC_p is the heat capacity change during the glass transition; T_m and ΔH_m are the melting temperature and enthalpy, respectively; and X_c is the crystalline fraction. The glass transition width (ΔT_g) is defined as the difference between onset and end of the glass transition process and reflects the number of relaxation processes associated with the glass transition. If the system exhibits microenvironments caused by dipole−dipole interactions, or hydrogen bonding, then this should undergo relaxation processes with different relaxation times, resulting in broadening of the glass transition.[20,21] Values of ΔT_g in the range of 10−25 °C are expected for semicrystalline homopolymers, as observed for PEO in Table 1.[22] ΔC_p values were determined assuming that the baselines before and after the glass transition were parallel. ΔC_p is associated with the changes in the degree of freedom in the glass transition, resulting from the free volume changes in this region, and reflects the changes of the conformational arrangement and, consequently, the changes in the entropy of the system. The T_m value (74 °C), most likely, does not correspond to the equilibrium melting temperature, but rather reflects morphological aspects (crystal size, defects on the

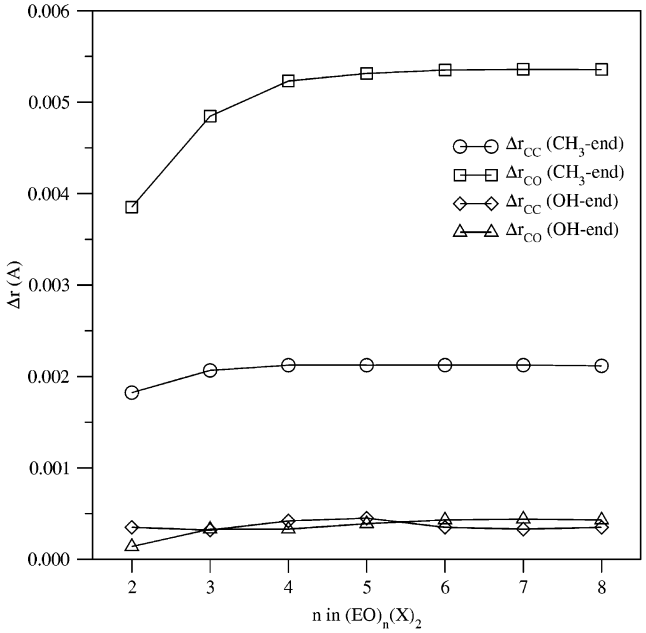

Figure 2. Dependence of the parameter Δr on the size of the oligomer chain (n).

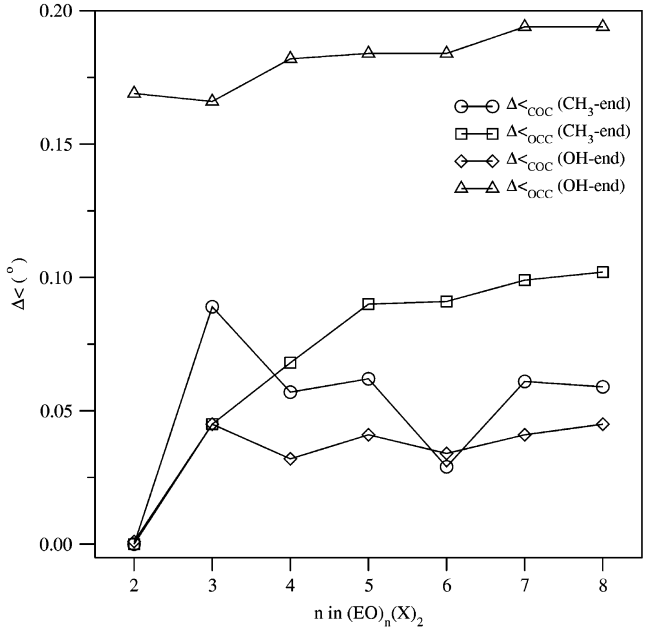

Figure 3. Dependence of the parameter $\Delta\angle$ on the size of the oligomer chain (n).

crystalline phase) and also thermodynamic aspects. Despite the influence of morphological analysis, this value is unequivocally associated with the melting of the crystalline fraction of PEO. From the area of the endothermic peak, associated with the melting of the crystalline phase, ΔH_m was evaluated and presented a value of 139 $J \cdot g^{-1}$ for the PEO sample. X_c was evaluated as described above and a value of 74% was found, associated with the amount of crystalline PEO in the sample. However, a crystalline PEO in equilibrium is hard to obtain, and thus, the DSC data are only representative of the sample treatment for the present case.

4.2. Convergence of the Electronic Structure and Properties with the Size (n) of the Oligomers. Geometry, energy, and vibrational modes of the $(EO)_n(X)_2$ oligomers ($n = 2-8$, $X = CH_3$, OH) provide parameters to be used as convergence criteria for the electronic structure dependence on the size (n) of the representative model systems, as shown in Figures 2−6. Geometric and electronic parameters were then defined in order to study the structural dependence of ethylene oxide oligomers on n.

The dependence of Δr_{CO} and Δr_{CC} on n for the $-CH_3$ and $-OH$ terminations are shown in Figure 2, where Δr_{CO} is the difference between the C−O bond lengths of the central atoms and border atoms of the chain, and Δr_{CC} is the difference between the C−C bond lengths of the central atoms and border atoms of the chain. The dependence of both Δr_{CC} and Δr_{CO} with n exhibited a strong border effect, on both the size of the oligomer and the termination used, but the absolute values of Δr represent less than 0.4% of the respective bond lengths. The values of Δr_{CO} for the hydroxyl-terminated oligomers were found to be higher than those for the methyl-terminated chain, and for this model system (the methyl-terminated one), the convergence of Δr is clearly observed for $n = 6$ (for both Δr_{CO} and Δr_{CC}).

The dependence of $\Delta\angle_{OCC}$ and $\Delta\angle_{COC}$ on n for the $-CH_3$ and $-OH$ terminations are shown in Figure 3, where $\Delta\angle_{OCC}$ and $\Delta\angle_{COC}$ are the differences (between center and border of the chain) of OCC and COC angles, respectively. For these parameters, low absolute values were found (less than 0.2%), similarly to Δr, but the dependence of $\Delta\angle$ with n exhibits a behavior different from that observed for bond lengths. The values of $\Delta\angle_{OCC}$ are higher for the hydroxyl-terminated oligomers than for the methyl-terminated ones, and for both terminations, no asymptotic behavior is clearly seen, despite the fact that low absolute values were found for $\Delta\angle$.

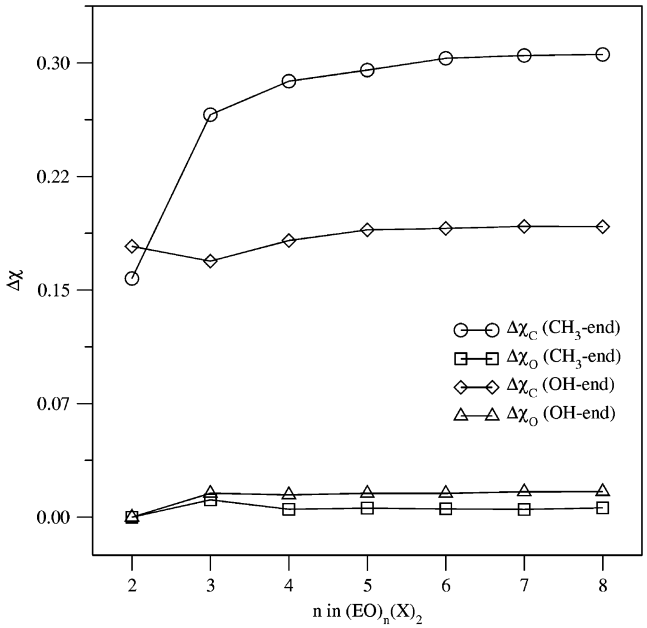

Figure 4. Dependence of the parameter $\Delta\chi$ on the size of the oligomer chain (n).

The analysis of the Mülliken charges on the atoms along the chain provides valuable information on the electronic structure of PEO. The dependence of $\Delta\chi$ on n for $-CH_3$ and $-OH$ terminations is shown in Figure 4, where $\Delta\chi_O$ and $\Delta\chi_C$ are the differences (between center and border of the chain) of Mülliken charges on oxygen and carbon atoms, respectively. Generally, $\Delta\chi_C$ presented higher values than $\Delta\chi_O$, due to a stronger electron localization on the oxygen atoms, which leads to smaller variations in the charge density compared to carbon atoms. $\Delta\chi_O$ and $\Delta\chi_C$ seem to converge for the $n = 6$ model system with both $-OH$ and $-CH_3$ terminations, and $\Delta\chi_C$ presented a smaller

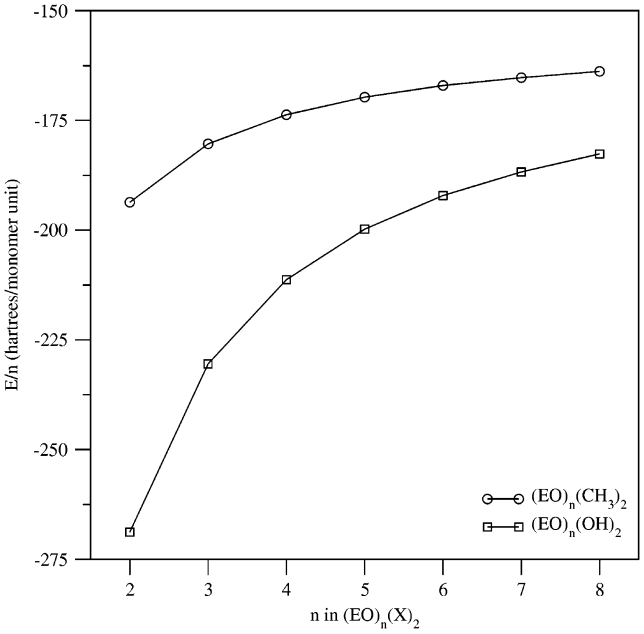

Figure 5. Total energy of the model systems divided by the number of monomer units (E/n) plotted against n.

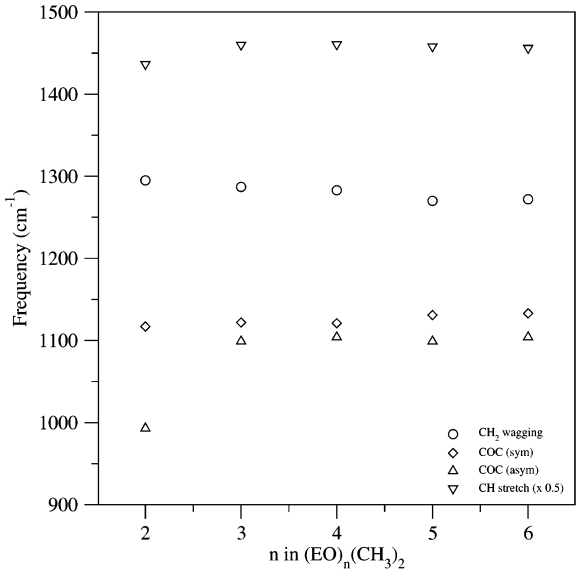

Figure 6. Frequency of selected calculated vibrational modes plotted against n.

variation with n for the hydroxyl-terminated oligomers, compared to the methyl-terminated ones.

In principle, the total energy (E) per unit cell (U) of a polymer U_∞ (E/n) can be obtained as the limit

$$\frac{E}{n} = \lim_{n\to\infty} \frac{E(U_nX_2)}{n} \tag{2}$$

i.e., by performing calculations for increasingly long oligomers U_nX_2, where the terminations have been saturated by X groups. However, in order to reduce finite size effects due to terminations, the energy change between two oligomers differing by a single unit cell can be employed:[23]

$$\frac{E}{n} = \lim_{n\to\infty} \Delta E_n = \lim_{n\to\infty}[E(U_{n+1}X_2) - E(U_nX_2)] \tag{3}$$

E/n can be interpreted as a monomeric density of energy, which should converge asymptotically as n rises. Usually, the

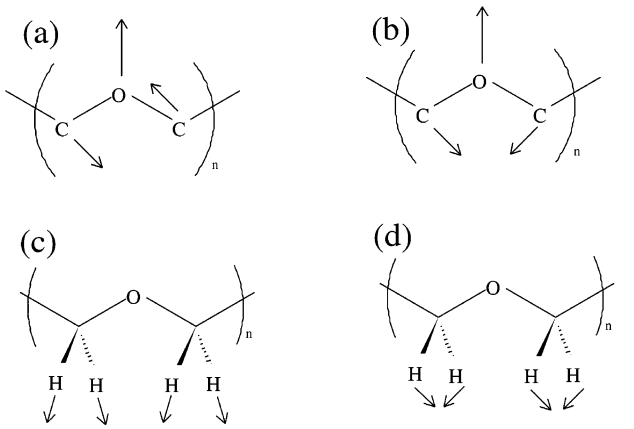

Figure 7. Displacement vectors for the vibrational modes: (a) COC (asym), (b) COC (sym), (c) CH (stretch), and (d) CH_2 (wagging). On (a) and (b) hydrogen atoms omitted for clarity.

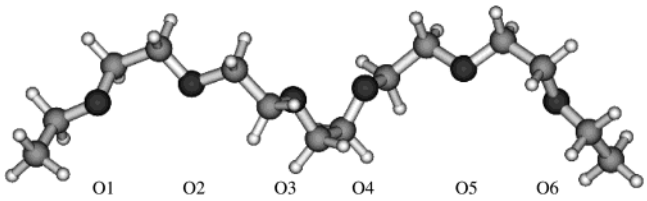

Figure 8. Model system of $(EO)_6(CH_3)_2$ in the helical conformation.

TABLE 2: Bond Lengths (d) and Relative Difference between Experimental and Calculated Values (Δ)

	exptl (Å)	calcd (Å)	Δ (%)
d_{CC} (border)	1.541 33	1.519 81	1.396 20
d_{CO} (O1)	1.423 60	1.417 06	0.459 40
d_{OC} (O1)	1.431 38	1.413 17	1.272 20
d_{CC}	1.533 87	1.515 63	1.189 15
d_{CO} (O2)	1.419 42	1.413 11	0.444 55
d_{OC} (O2)	1.441 73	1.413 97	1.925 46
d_{CC}	1.531 76	1.515 97	1.030 84
d_{CO} (O3)	1.416 42	1.414 00	0.170 85
d_{OC} (O3)	1.428 95	1.413 81	1.059 52
d_{CC}	1.541 97	1.515 43	1.721 17
d_{CO} (O4)	1.423 91	1.413 93	0.700 89
d_{OC} (O4)	1.432 08	1.413 41	1.303 70
d_{CC}	1.542 60	1.515 33	1.767 79
d_{CO} (O5)	1.424 86	1.413 45	0.800 78
d_{OC} (O5)	1.429 11	1.412 99	1.127 97
d_{CC}	1.546 99	1.515 66	2.025 22
d_{CO} (O6)	1.428 79	1.413 46	1.072 94
d_{OC} (O6)	1.436 02	1.417 63	1.280 62
d_{CC} (border)	1.528 93	1.519 60	0.610 23

finite model cluster is simply constructed by using hydrogen atoms as chain terminators. A unit cell in the middle of such an oligomer is assumed to be virtually in the same environment as a corresponding unit cell in a polymer of infinite length, especially when only the rather short range electron correlation effects are important to the description of the system.[24] The effect of the chain termination can be clearly seen in the convergence of E/n against n in Figure 5. For the hydroxyl-terminated oligomers, model systems with seven and eight monomer units still present a considerable variation of E/n, while for the methyl-terminated system this parameter practically converges after six units. This feature reflects the effect of the termination groups on the electronic structure of the oligomers and, consequently, on the total energy of the system.

The effect of the oligomer size (n) on the simulated vibrational spectrum can be monitored as shown in Figure 6, where selected vibrational modes calculated for the linear $(EO)_n(CH_3)_2$ model system are plotted against n. The modes shown

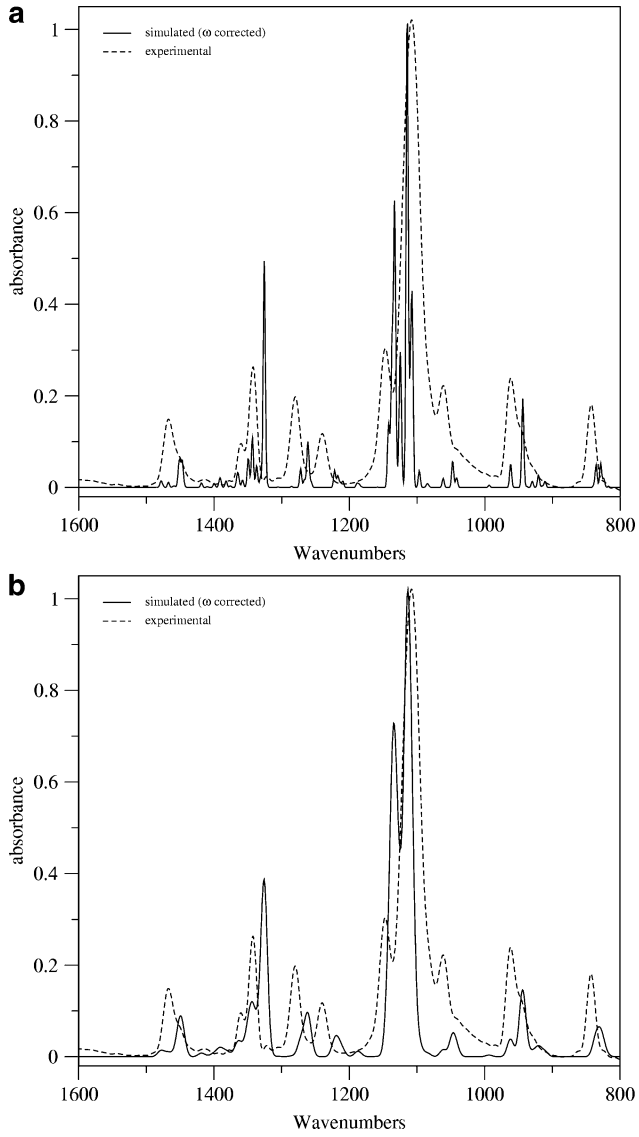

Figure 9. (a) Experimental and simulated ("high resolution") vibrational spectra in the 800−1600 cm^{-1} region. (b) Experimental and simulated ("low resolution") vibrational spectra in the 800−1600 cm^{-1} region [1].

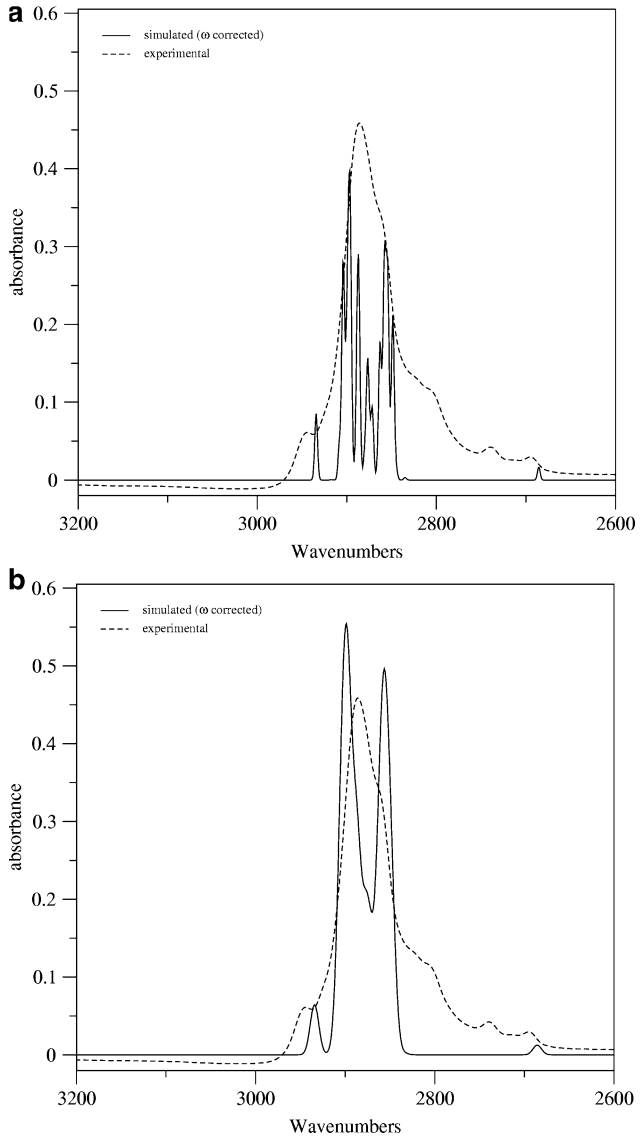

Figure 10. (a) Experimental and simulated ("high resolution") vibrational spectra in the 3200−2600 cm^{-1} region. (b) Experimental and simulated ("low resolution") vibrational spectra in the 3200−2600 cm^{-1} region.

in Figure 6 were chosen as representative of localized vibrations, which are less susceptible to chain length and border effects. In Figure 7, the calculated displacement vectors are shown for the vibrational modes: (a) COC (asym), (b) COC (sym), (c) CH (stretch), and (d) CH_2 (wagging). The calculated frequencies for these modes gradually approach a constant value with increasing n. The frequency values, as E/n, should converge for $n \rightarrow \infty$, but still would not be representative of the vibrational spectrum of PEO, since this (the experimental spectrum) is a sum of a large number of different chain conformer spectra. One interesting feature in these spectra is that some of the most characteristic vibrational modes of PEO are present even in the smaller oligomers ($n = 2$), but obviously shifted to different frequencies, due to a series of factors, which include border and chain length effects, chain confinement and medium not considered in the calculations, contributions of other chain conformations, and specific anharmonic corrections to the vibrational modes (not calculated explicitly, only included as a linear correction factor).

4.3. Geometry of $(EO)_6(CH_3)_2$. The optimized geometry of the helical conformer $(EO)_6(CH_3)_2$ with B3LYP hybrid functional and 6-31G(d,p) basis set is represented in Figure 8, and the relative difference between selected experimental[25] and calculated parameters is shown in Table 2. The border effect seems to be less important for the molecular structure, considering the difference of bond lengths in the center and near the terminations of the molecule. This is also related to the fact that a large number of conformers can be found as local minima for a highly flexible molecule such as oligo(ethylene oxide). In the work of Takahashi,[25] the experimental data were obtained from single-crystal X-ray diffraction and represent mean values of atomic positions. Additionally, hydrogen atoms do not exhibit diffraction patterns and were generated by an algorithm. Since the difference in bond lengths in the main chain (C−O and C−C bonds) is less than 2.02522%, the theoretical results can be considered to be in very good agreement with the experimental data.

The gauche effect in PEO was investigated by Müller-Plathe and Gunsteren,[26] utilizing quantum mechanical methods in dimethoxyethane as a molecular model system, for calculations in the gas phase and with a continuum cavity. According to the authors, the gauche conformation of dimethoxyethane and, for instance, of PEO, is caused by the presence of a polarizable medium and not by any internal molecular effect. The experi-

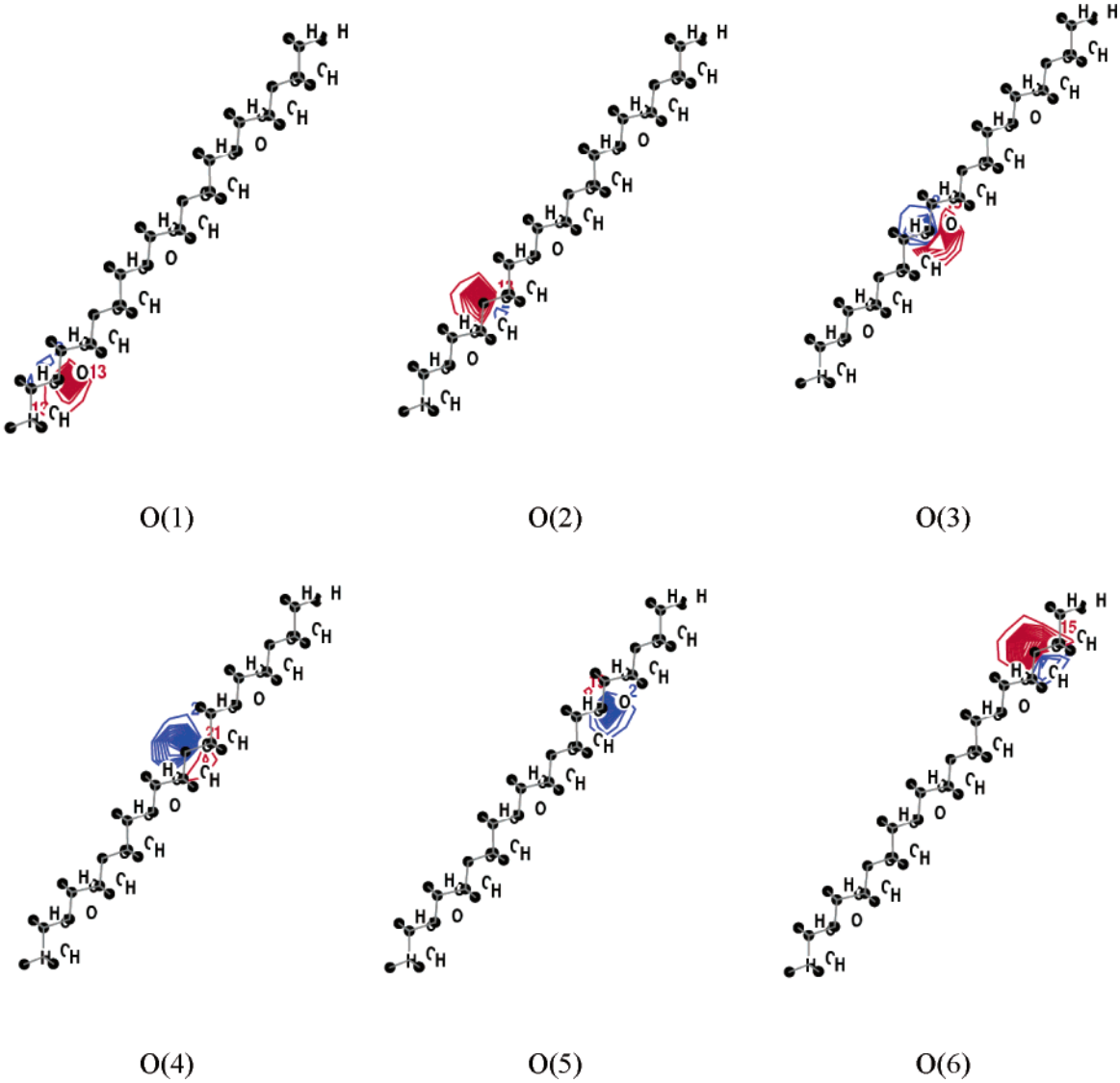

Figure 11. Plots of localized orbitals at the oxygen atoms obtained with F−B and E−R methods for linear $(EO)_6(CH_3)_2$ model systems.

mental fact is, however, that PEO, as many other semicrystalline polymers, presents a solid-state structure that consists of a mixture of a helical conformer (70−85%) and other conformers, including the linear one.[27]

In the present work, we describe the vibrational spectrum of PEO as a weighted sum of spectra of different conformers, and the electronic structure of the polymer utilizing oligomer model systems. The description of PEO and the intermolecular interactions involving the electron-rich oxygen atoms in the chain, as well as the vibrational spectrum of interacting systems (such as polymer blends, polymeric electrolytes, and composites), can be performed utilizing the method described here. The main advantage of this is the possibility of a high level wave function description of localized molecular properties.

4.4. Vibrational Spectrum of Poly(ethylene oxide). Experimental vibrational spectra of PEO and the weight-summed spectra of linear and helical model systems $(EO)_6(CH_3)_2$ are shown in the two different spectral regions, 1600−800 and 3200−2600 cm^{-1}, in Figures 9 and 10, respectively. From the high resolution theoretical spectrum (Figures 9a and 10a), it is possible to describe a set of vibrational modes which contribute to the observed experimental band, composed of several unresolved peaks. These modes arise both from the linear and the helical model conformers, and the application of weights related to the crystalline and noncrystalline fractions allows the simulation of the vibrational spectrum of PEO with good agreement.

The refinement of the description of the infrared spectra involving two $(EO)_6(CH_3)_2$ conformations (helical and linear) was carried out by analyzing the vibrations of the isolated molecules and excluding the modes which involve the methyl end groups, in order to avoid border effects that could compromise the results of the simulated spectra. There were 27 and 33 vibrational modes associated with border effects in the linear and helical conformers, respectively. One of the characteristics of vibrational spectra of semicrystalline polymers is the contribution of several different chain conformations to the observed peaks, which are not always clearly interpreted. The utilization of model systems does not cover the entire range of possible chain conformations, but is one step forward in the interpretation of the vibrational spectra of semicrystalline polymers.

Figure 9a exhibits the individual peaks related to localized vibrational modes such as ν(C−O) to more anharmonic modes involving up to 12 atoms in the main chain. The increase in line width causes a match in the number of peaks, comparing the theoretical and experimental spectra, despite the frequency shifts observed. In the spectral region from 1600 to 800 cm^{-1},

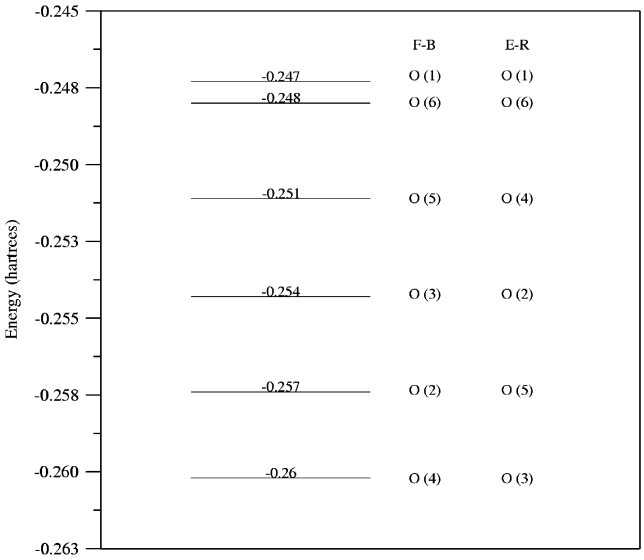

Figure 12. Energy values and attribution of localized molecular orbitals of oxygen atoms in the linear $(EO)_6(CH_3)_2$ model system based on F−B and E−R methods.

the similarity between the theoretical and experimental spectra was enhanced with the increase in the line width. Many vibrational modes which appear to be individual peaks contributed to a single broad absorption band when the "resolution" was lowered, and the intensities became much closer to the experimental values, showing very good agreement between theoretical and experimental spectra.

In Figure 10a, 13 peaks can be seen at the resolution used, but in fact, there are 36 modes (from both linear and helical conformers), contributing to the observed spectrum, all relative to the CH_2 group vibrations. When the "resolution" is lowered, however, there is a overestimation of the spectrum intensity due to overlapping of individual broadened peaks as shown in Figure 10b.

4.5. Electronic Structure of Ethylene Oxide Oligomers. One of the most interesting properties of PEO, which makes it a suitable polymer matrix for technological applications, is the capability for dissolving high amounts of alkali metal salts. These polymer−salt systems, also called solid electrolytes, have been studied by means of ab initio calculations, where the main interest was to describe the coordination of the metal ion, especially lithium, by the polymeric matrix.[28,29] However, a more detailed description of the wave function of PEO has not been reported in the literature to our knowledge.

Concerning the atomic centers available for the interactions with metal salts, the oxygen atoms are the preferred sites, as described by Bruce and co-workers,[30] Baboul and co-workers,[31] and Johansson.[10] The localization of molecular orbitals allows the interpretation of the wave function of the molecular system under study in a more detailed way. For the $(EO)_6(CH_3)_2$ model system, both F−B and E−R methods gave similar results, concerning the shape of the localized orbitals at the oxygen atoms, as can be seen in Figure 11. Each oxygen atom presents a well-defined electron density, which is not overlapped with the electron density from other neighbor atoms. These frontier orbitals present occupation of two electrons each, and then justifying the observed interactions (both experimental and theoretical) with cations, as expected. However, these orbitals do not present the same energy, as shown in Figure 12. A comparison between the localized orbitals of the different model systems $(EO)_n(CH_3)_2$ shows a strong influence of n on the energy values and on the energy difference between the oxygen atoms at the border and the center of the chain. Comparatively to other cation-coordinating solvents such as water, the energy difference of the localized orbitals is about 0.06−0.08 hartree, varying with the chain length. The model systems currently employed in the description of PEO−salt systems are usually composed of diglyme,[31] tetraglyme, pentaglyme, and hexaglyme[29] complexes with Li^+, which, based on our present results, are models that may be refined by the utilization of oxygen atoms in the middle of an oligomer chain of, at least, six monomer units. The utilization of oxygen atoms at the borders of the oligomer chain may induce systematic errors due to the differentiated energy of these doubly occupied orbitals.

5. Conclusion

The finite size cluster approach has proved to be an appropriate tool for vibrational spectrum and electronic structure calculations of PEO, and the utilization of oligo(ethylene oxide) model systems with six monomer units was shown to be a good approximation for the simulation of PEO molecular localized properties. The method proposed for the simulation of the vibrational spectrum of PEO based on the weight-summed theoretical spectra of linear and helical model systems is a step forward in the simulation of vibrational spectra of semicrystalline polymers. The detailed theoretical vibrational study of macromolecules such as PEO provides a valuable tool for the description of polymer electrolytes, polymer blends, and composites, with localized, high level wave function methods. The electronic structure calculations with localized orbitals allowed a more detailed description of the wave function and showed a not negligible border effect on the electronic properties of the model system under study. This is specially important in the description of intermolecular interactions involving the electron-rich oxygen atoms in the PEO chain.

Acknowledgment. The authors thank the State of Rio de Janeiro Foundation for Research Support (FAPERJ, Grant E-26/170414/2000) for support of this work and the Brazilian National Research Council (CNPq) for fellowships.

References and Notes

(1) Martin-Litas, I.; Andreev, Y. G.; Bruce, P. G. *Chem. Mater*. **2002**, *14*, 2166.
(2) Murata, K.; Izuchi, S.; Yoshihisa, Y. *Electrochim Acta* **2000**, *45*, 1501.
(3) De Paoli, M.-A.; Zanelli, A.; Mastragostino, M.; Rocco, A. M. *J. Electroanal. Chem.* **1997**, *435*, 217.
(4) Rocco, A. M.; Fonseca, C. P.; Pereira, R. P. *Polymer* **2002**, *43*, 3601.
(5) Salomon, M.; Xu, M.; Eyring, E. M.; Petrucci, S. *J. Phys. Chem.* **1994**, *98*, 8234.
(6) Rocco, A. M.; Bielschowsky, C. E.; Pereira, R. P. *Polymer* **2003**, *44*, 361.
(7) Li, X.; Hsu, S. L. *J. Polym. Sci., Polym. Phys. Ed.* **1984**, *22*, 1331.
(8) Borodin, O.; Smith, G. D. *J. Phys. Chem. B* **2003**, *107*, 6801 and references therein.
(9) *Solid State Electrochemistry*; Bruce, P. G., ed.; Cambridge University Press: Cambridge, 1997.
(10) Johansson, P. *Polymer* **2001**, *42*, 4367.
(11) Johansson, P.; Tegenfeldt, J.; Lindgren, J. *Polymer* **2001**, *42*, 6573.
(12) Krishnan, M.; Balasubramanian, S. *Phys. Rev. B* **2003**, *68*, 064304.
(13) Cimmino, S.; Dipace, E.; Martuscelli, E.; Silvestre, C. *Makromol. Chem.* **1990**, *191*, 2447.
(14) Becke, A. D. *J. Chem. Phys.* **1993**, *98*, 5648.
(15) Schmidt, M. W.; Baldridge, K. K.; Boatz, J. A.; Elbert, S. T.; Gordon, M. S.; Jensen, J. H.; Koseki, S.; Matsunaga, N.; Nguyen, K. A.; Su, S. J.; Windus, T. L.; Dupuis, M.; Montgomery, J. A. *J. Comput. Chem.* **1993**, *14*, 1347.
(16) Boys, S. F. In *Quantum Theory of Atoms, Molecules, and Solids*; Lowdin, P. O., Ed.; Academic Press: New York, 1966; pp 253−266.
(17) Edmiston, C.; Ruedenberg, K. *Rev. Mod. Phys.* **1963**, *35*, 457.
(18) Scott, A. P.; Radom, L. *J. Phys. Chem.* **1996**, *100*, 16502.

(19) Scilab Group. Scilab2.7. *Introduction to Scilab—User's Guide*; http://www-rocq.inria.fr/scilab.
(20) Li, X.; Hsu, S. L. *J. Polym. Sci., Polym. Phys.* **1984**, *22*, 1331.
(21) Rocco, A. M.; Moreira, D. P.; Pereira, R. P. *Eur. Polym. J.* **2003**, *39*, 1925.
(22) Rocco, A. M.; Bielschowsky, C. E.; Pereira, R. P. *Polymer* **2003**, *44*, 361.
(23) Abdurahman, A.; Albrecht, M.; Shukla, A.; Dolg, M. *J. Chem. Phys.* **1999**, *110*, 8819.
(24) Abdurahman, A.; Shukla, A.; Dolg, M. *Chem. Phys.* **2000**, *257*, 301.
(25) Takahashi, Y.; Tadokoro, H. *Macromolecules* **1973**, *6*, 672.
(26) Müller-Plathe, F.; van Gunsteren, W. F. *Macromolecules* **1994**, *27*, 6040.
(27) Tadokoro, H. *Polymer* **1984**, *25*, 147.
(28) Kříž, J.; Abbrent, S.; Dybal, J.; Kurková, D.; Lindgren, J.; Tegenfeldt, J.; Wendsiö, Å. *J. Phys. Chem. A* **1999**, *103*, 8505.
(29) Johansson, P.; Tegenfeldt, J.; Lindgren, J. *Polymer* **1999**, *40*, 4399.
(30) MacGlashan, G. S.; Andreev, Y. G.; Bruce, P. G. *Nature* **1999**, *398*, 792.
(31) Baboul, A. G.; Redfern, P. C.; Sutjianto, A.; Curtiss, L. A. *J. Am. Chem. Soc.* **1999**, *121*, 7220.